Technologies Enabling Ultrafast Short-Reach Transmission

Qian Hu
Nokia Bell Labs, 600 Mountain Ave, Murray Hill, NJ 07974, USA
qian.hu@nokia-bell-labs.com

Abstract: This paper reviews technologies for ultrahigh symbol rate transmission in short-reach optical links, including high-speed signal generation and sampling, broadband optical signal modulation, as well as advanced digital signal processing. © 2024 The Author(s)

1. Introduction

The preferred technical solutions for short-reach datacenter interconnects (DCIs) with a distance up to a few kilometers are based on intensity modulation and direct detection (IM/DD) because of their simple implementation, low power consumption and compatibility with demanding cost targets of datacom. To further increase the data rate in short-reach DCIs, data transmission at higher symbol rates is desired, so that the number of optical components, such as lasers, modulators and photodetectors, as well as their power consumption, can be kept low. Further symbol rate increase poses following challenges for short-reach transmission systems. (1) Electrical subsystems, in particular digital-to-analog converters (DACs)/analog-to-digital converters (ADCs) need to provide sufficient analog bandwidths and sampling rates to support generation and sampling of analog signals at high symbol rates. (2) Optoelectronic subsystems: modulators/photodetectors need to have broad electrical-to-optical (EO)/optical-to-electrical (OE) bandwidths to allow modulation and detection of high-symbol rate optical signals. (3) An increase in symbol rate also presents a challenge to digital signal processing (DSP), which is applied to compensate signal distortions induced by bandwidth limitation, and to support advanced modulation format decoding and forward error correction. In this paper, we review several technologies that can be employed to overcome challenges associated with high-symbol rate transmission, thus enabling ultrafast short-reach IM/DD communication.

2. Ultrahigh-Symbol Rate Signal Generation and Sampling

DACs and ADCs are the interfaces between the analog electrical signals and the digital signal processing circuits employed in many modern optical transmission systems. Generation and sampling of electrical signals at high symbol rates require broadband operation and fast sampling DACs and ADCs. Complementary metal-oxide semiconductor (CMOS) technology, known for its high yield, low cost and low power consumption, has been widely used for commercial DACs and ADCs. As the process node size progressively decreases, the analog bandwidth and sampling rate continue to increase, which is manifested by the increase in symbol rates used in optical transmission systems over the years. Nevertheless, as the node size shrinks to single nanometers, transistors become dominated by quantum effects, which may result in slowing down the progress of CMOS bandwidth scaling in the future.

Concepts of analog multiplexer (AMUX) and analog demultiplexer (ADeMUX) manufactured in a broadband technology, such as InP or SiGe, have been proposed to complement DACs or ADCs by extending analog bandwidth beyond limitations of CMOS. Figs. 1(a,b) illustrate the operating principle of the AMUX and the ADeMUX. The AMUX operates as a high-speed switch controlled by a clock signal, interleaving analog waveforms from N parallel DACs (N=2 in Fig. 1) [1-3]. The interleaved output has N times the symbol rate of the inputs. The ADeMUX operates in the reverse direction, deinterleaving a high-speed input signal into N parallel waveforms [4,5]. The deinterleaved outputs have $1/N$ times the symbol rate of the input, relaxing the bandwidth requirement for the subsequent parallel bank of ADCs. The AMUX/ADeMUX can be monolithically integrated with driver amplifiers/transimpedance amplifiers in the same technology. Therefore, the component count and integration complexity are not negatively impacted.

In [6], we used a SiGe AMUX chip, shown in Fig. 1(c), for ultrahigh-symbol rate IM/DD transmission employing pulse amplitude modulation (PAM). The AMUX chip is manufactured in 130 nm technology SG13G3 of IHP. Using this AMUX chip, 176 GBd PAM-8 transmission was successfully demonstrated. Figs. 1(d,e) show eye diagrams of

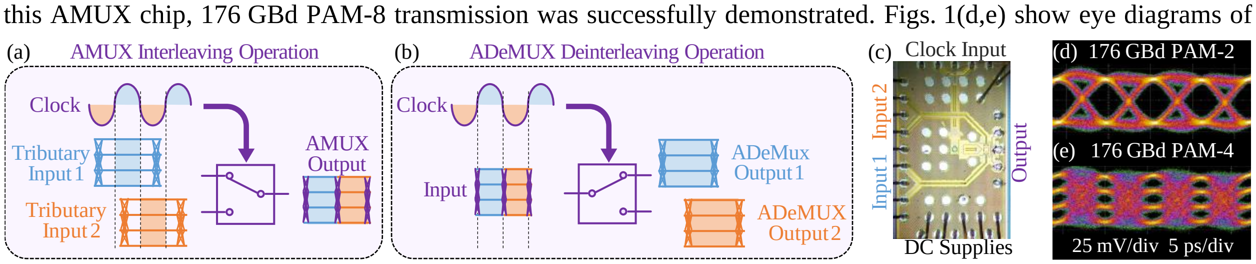

Fig. 1 Diagrams showing: (a) interleaving operation of a 2:1 AMUX, and (b) deinterleaving operation of a 1:2 ADeMUX. (c) Photo of a SiGe AMUX chip. Eye diagrams of electrical signals at 176 GBd: (d) PAM-2, (e) PAM-4.

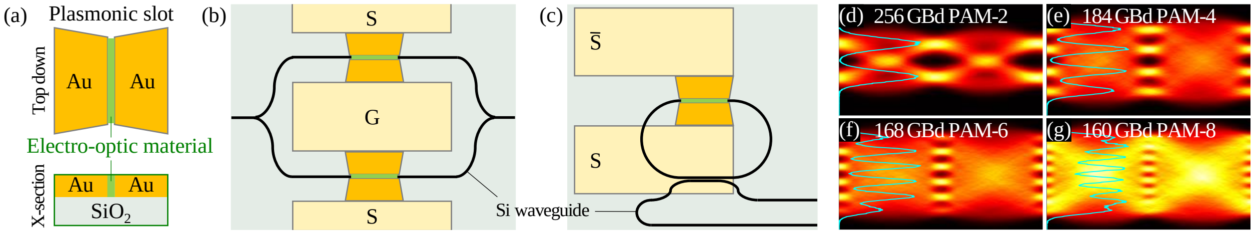

Fig. 2 Schematics of (a) plasmonic nanostructure, (b) plasmonic MZM and (c) plasmonic RRM. (d-g) Post-equalizer eye diagrams for a plasmonic RRM-based IM/DD system.

electrical signals obtained at the AMUX output when digital transmitter pre-emphasis was applied. SNR as high as 21 dB was achieved, demonstrating broad bandwidth of the AMUX circuit and excellent linearity appropriate for multilevel PAM transmission.

3. Broadband Optical Signal Modulation

Silicon photonics leverages maturity of CMOS manufacturing technology, enabling low-cost production of high density photonic integrated circuits implementing complex optical functionalities. It provides attractive solution for optical co-packaging with switch ASICs to shorten electrical paths, thus bringing significant improvements to analog bandwidth and power efficiency. Silicon photonic modulator serves as an important building block of co-packaged optics. A broad EO bandwidth is essential to support ultrahigh-symbol rate transmission. Silicon modulators based on free-carrier plasma dispersion effect have advantages of small footprint, low insertion loss and easy fabrication, however they face challenges in further improvement of modulation efficiency and EO bandwidth.

Plasmonic modulators can be seamlessly integrated into the silicon photonics platform at the last step of the standard process flow [7], providing significantly broader EO bandwidth compared to silicon modulators. Plasmonic modulators use a metal wall-insulator-metal wall structure to guide light [8], where the metallization serves at the same time as electrical contacts. Schematic of a plasmonic nanostructure is shown in Fig. 2(a). It has the following advantages: (1) an extremely compact footprint, leading to an efficient use of expensive wafer real estate; (2) a tight confinement for both optical and electrical fields resulting in a high modulation efficiency; (3) a small RC constant contributing to an ultrabroad EO bandwidth.

We have experimentally explored the potential of plasmonic modulators to realize ultrahigh-symbol rate optical transmission. In [9], we employed a plasmonic Mach-Zehnder modulator (MZM) with a schematic shown in Fig. 2(b) in a short-reach optical link, demonstrating a symbol rate up to 144 GBd for PAM-8 signaling, up to 156 GBd for PAM-4 and more than 300 GBd for tetrabinary. For plasmonic MZMs, high insertion loss remains a major challenge. This can be circumvented by using a ring resonator structure. Fig. 2(c) shows schematic of a plasmonic ring resonator modulator (RRM). In [10], we employed such modulator and successfully demonstrated 160 GBd PAM-8, 168 GBd PAM-6, 186 GBd PAM-4 and 256 GBd PAM-2 transmission. Eye diagrams at the output of the receiver equalizer are shown in Figs. 2(d-g).

4. Digital Signal Processing for Ultrahigh-Symbol Rate Signaling

Electrical and optical components exhibit low-pass frequency characteristics and thus induce harmful inter-symbol interference (ISI). The transmitter DSP often compensates for its own low-pass response using a pre-emphasis filter, which results in enhancement or peaking of high frequencies. Such pre-emphasis usually leads to a reduction in the average power of the generated electrical signal, which decreases the resulting optical modulation amplitude (OMA). The receiver DSP compensates for the low-pass response using an equalizer, which in turn induces equalization-enhanced noise. To avoid these effects, a partial-response-encoded (PR-encoded) signal with a low-pass spectral envelope can be applied, which can efficiently increase the OMA and reduce the equalization-enhanced noise. Moreover, the PR encoding significantly reduces the effective signal bandwidth, reducing the impairments due to the system bandwidth limitation [8,9,11].

To shape the signal spectrum, the PR encoder induces short and controlled ISI into the data symbols. Different approaches can be used for symbol decoding. One approach is to use trellis-based decoder, which computes the transition metric based on the symbols affected by the ISI. Such decoding method is characterized by high computational complexity. Especially, the trellis size increases fast with the memory length and the number of levels. Alternatively, a decision feedback equalizer can be used. It removes the ISI if correct symbol decision is made. However, a wrong symbol decision can cause a burst of errors. Such error propagation can be avoided by implementing the feedback structure at the transmitter side instead, which is referred to as a precoder [12-16].

Fig. 3(a) illustrate the schematic of precoding, encoding and decoding in a system employing PR-encoded signals. The figure demonstrates a case using a $(1+D)$ PR filter, which can be further generalized. The precoder and the encoder

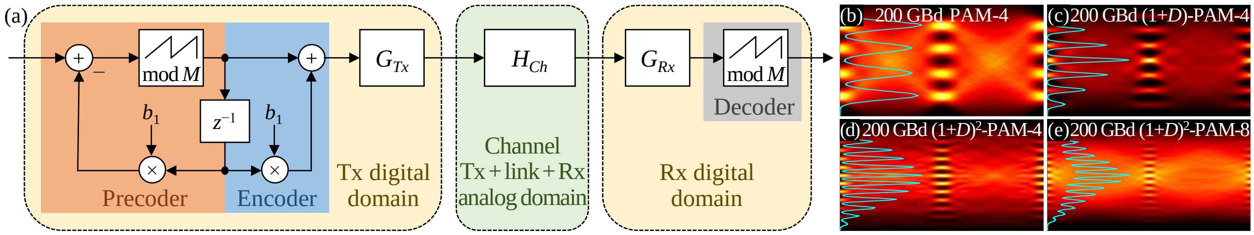

Fig. 3 (a) Schematic of the precoding, encoding and decoding of the PR modualtion. Post-equalizer eye diagrams at 200 GBd: (b) PAM-4, (c) (1+D)-encoded PAM-4, (d) (1+D)^2-encoded PAM-4 and (e) (1+D)^2-encoded PAM-8.

together produce a signal that exhibits a low-pass spectral envelope (spectral shaping) but is free from ISI. To recover the M-level PAM symbols, the decoder only uses a slicer and modulo operation. Spectral shaping introduced by the concatenation of the encoder filter and the pre-emphasis filter G_{Tx} effectively reduces enhancement of high frequency components, resulting in an increased OMA in a peak power constrained system. In such system, the impact of pre-emphasis on OMA is small even when the pre-emphasis filter G_{Tx} is the inverse of the channel response H_{ch}. As a result, the frequency response of the receiver equalizer G_{Rx} is approximately flat, avoiding equalization-enhanced noise.

In [17], we experimentally demonstrated improved performance in terms of bit error ratio, mutual information and net bitrate using PR encoded signals. Figs. 3(b-d) shows the post-equalizer eye diagrams of PAM-4, (1+D)-encoded PAM-4 and (1+D)^2-encoded PAM-4 signals at 200 GBd. Compared to PAM-4, SNR is improved for both (1+D)-encoded and (1+D)^2-encoded PAM-4. However, an increase in the number of amplitude levels partly curtails the benefit of the increased SNR for (1+D)^2-encoded PAM-4. The best tradeoff is achieved with (1+D) encoding. Fig. 3(e) shows the post-equalizer eye diagram of 200 GBd (1+D)-encoded PAM-8, resulting in a net bitrate of 510.6 Gbit/s.

5. Conclusions

In this paper, we review enabling technologies for ultrahigh-symbol rate transmission in short-reach IM/DD systems. We review the concept of AMUX and ADeMUX and their capabilities to extend the analog bandwidth and sampling rate offered by CMOS DACs and ADCs for ultrahigh-symbol rate signal generation and sampling. We also review plasmonic modulators on silicon photonics platform, which have advantages of compact footprint, high modulation efficiency and ultrabroad EO bandwidth. Finally, we review the digital signal processing employing partial response encoding, revealing its potential to improve the performance of ultrahigh-symbol rate transmission systems.

6. References

[1] Q. Hu *et al.*, "120 GSa/s BiCMOS analog multiplexer enabling 360 Gbit/s DSCM-PCS-256QAM IM/DD transmission," Proc. OFC 2021, paper F2D.1, doi: 10.1364/OFC.2021.F2D.1.
[2] Q. Hu *et al.*, "120 GSa/s BiCMOS AMUX for 360 Gbit/s High-Information-Rate Signal Generation Demonstrated in 10 km IM/DD System," JLT **40**, 1330-1338 (2022), doi: 10.1109/JLT.2021.3133409.
[3] Q. Hu *et al.*, "128 GSa/s SiGe Analog Multiplexer Enabling PDM-DSCM-PCS-256QAM Transmission over 80 km SSMF," in Proc. APC 2022, paper SpTh1I.6, doi: 10.1364/SPPCOM.2022.SpTh1I.6.
[4] K. Schuh *et al.*, "High-speed IM/DD transmission with analog (de-)multiplexers," Proc. ECOC 2021, pp. 831-834, doi: 10.1109/ECOC52684.2021.9606116.
[5] P. Thomas *et al.*, "1-to-4 Analog Demultiplexer With up to 128 GS/s for Interleaving of Bandwidth-Limited Digitizers in Wireline and Optical Receivers," IEEE JSSC **56**, 2611-2623 (2021), doi: 10.1109/JSSC.2021.3100677.
[6] Q. Hu *et al.*, "467 Gbit/s Net Bitrate IM/DD Transmission Using 176 GBd PAM-8 Enabled by SiGe AMUX with Excellent Linearity," submitted to OFC 2024.
[7] C. Hoessbacher *et al.*, "System-on-Chip Photonic Integrated Circuits in Silicon Photonics and the Role of Plasmonics," Proc. OFC 2023, paper Tu2E.5. doi: 10.1364/OFC.2023.Tu2E.5.
[8] Q. Hu *et al.*, "Plasmonic-MZM-based Short-Reach Transmission up to 10 km Supporting >304 GBd Polybinary or 432 Gbit/s PAM-8 Signaling," Proc. ECOC 2021, pp. 1214-1217, doi: 10.1109/ECOC52684.2021.9606060.
[9] Q. Hu *et al.*, "Ultrahigh-Net-Bitrate 363 Gbit/s PAM-8 and 279 Gbit/s Polybinary Optical Transmission Using Plasmonic Mach-Zehnder Modulator," JLT **40**, 3338-3346 (2022), doi: 10.1109/JLT.2022.3172246.
[10] Q. Hu *et al.*, "Up to 256 GBd PAM Transmission Using Plasmonic Ring Resonator Modulator," Proc. ECOC 2023, paper We.B.6.2.
[11] R. Borkowski *et al.*, "Experimental Evaluation of PAM and Polybinary Modulation for Intra-DCI Optical Lanes with up to 300 Gbit/s Net Bitrates," Proc. OFC 2022, paper M4H.6, doi: 10.1364/OFC.2022.M4H.6.
[12] Q. Hu *et al.*, "High data rate Tomlinson-Harashima-precoding-based PAM transmission," Proc. ECOC 2019, pp. 495-498, doi: 10.1049/cp.2019.0869.
[13] Q. Hu *et al.*, "Up to 94 GBd THP PAM-4 Transmission with 33 GHz Bandwidth Limitation," Proc. ECOC 2018, pp. 1396-1398, doi: 10.1109/ECOC.2018.8535334.
[14] Q. Hu *et al.*, "IM/DD Beyond Bandwidth Limitation for Data Center Optical Interconnects," in JLT **37**, 4940-4946 (2019), doi: 10.1109/JLT.2019.2926218.
[15] Q. Hu *et al.*, "84 GBd Faster-Than-Nyquist PAM-4 Transmission Using Only Linear Equalizer at Receiver," Proc. OFC 2019, paper W4I.2, doi: 10.1364/OFC.2019.W4I.2.
[16] Q. Hu *et al.*, "50 Gb/s PAM-4 Transmission Over 80-km SSMF Without Dispersion Compensation," Proc. ECOC 2018, pp. 1019-1021, doi: 10.1109/ECOC.2018.8535179.
[17] Q. Hu and R. Borkowski, "510 Gbit/s Net Bitrate IM/DD Link Enabled by 200 GBd Precoded Duooctonary (1+*D*)-PAM-8 Modulation with Memoryless Decoding," Proc. ECOC 2023, paper Th.C.1.7.